EPR and resonant cavity measurements of free electrons and metastable N atoms produced in a He-N$_2$ microwave discharge

Enrique López-Moreno*

Facultad de Ciencias, Universidad Nacional Autónoma de México,
Circuito Exterior, Ciudad Universitaria,
04510 México, D.F.

V. Beltrán-López*

Instituto de Ciencias Nucleares, Universidad Nacional Autónoma de México,
Circuito Exterior, Ciudad Universitaria,
Apartado postal 70-543, 04510 México, D.F., México.

Abstract. Metastable N(^2D) atoms and free electrons in the afterglow of a microwave discharge in a He-N$_2$ gas stream were observed, by means of EPR. Free electron densities were measured by resonance frequency shifts in the spectrometer X-band cavity.

The decay of free electron density with distance in the afterglow of a pure helium discharge at 363 K was measured at pressures above 6.5 kPa. He$_2^+$ is shown to predominate over He$^+$ in the afterglow by the value obtained from these measurements for the ambipolar diffusion constant.

The free electron density is observed to decay in the afterglow as N$_2$ is added to the gas stream, and measured as a function of N$_2$ flow. Strong EPR signals of N(^2D) are observed around 5% nitrogen partial pressure. Production of N(^2D) by reactions He$_2^+$ + N$_2$ $\rightarrow$ 2He + N$_2^+$ followed by N$_2^+$ + e $\rightarrow$ N* + N, is evidenced by these measurements.

PACS: 33.35.Ex; 52.80.Tn; 52.80.Yr

1. Introduction

EPR has often been used to study the products of electrical discharges in static and in flowing afterglows. This technique has the advantage of negligible interference with gas kinetics and with interaction processes occurring in the gaseous samples. It has provided many rate constants for several reactions via relative concentration measurements in kinetic flow systems [1-3]. Information on the structure of atomic and free radical species has been obtained from spectral analysis [4,5,6].

*Miembro del SNI.

EPR has also been used to study metastable atomic states since $N(^2D)$ was first detected by this technique [7,8,9]. It provides an interesting tool to study the formation of metastable atomic nitrogen because it can also detect coexisting electrons; either, by microwave absorption at the cyclotron resonance field or by the shift of the X-band resonant frequency induced by the electron charges [10,11]. The last technique has the additional advantage of being usable at any magnetic field and capable of yielding reliable measurements of the charge density.

In this work, we describe the use of an EPR spectrometer to study the reaction mechanisms leading to the production of metastable atomic nitrogen in the afterglow of a microwave discharge in He-N_2. The molecular helium ion, predominantly present in the helium discharge afterglow in our operating conditions, is identified by the value obtained for the ambipolar diffusion coefficient from measurements of the decay of electron charge density along the tube. The density values are obtained from the shifts in the X-band cavity resonant frequency induced by the electron charges. We give formulae for these calculations, appropriate to a rectangular cavity traversed by a cylindrical flow tube and for a parabolic velocity distribution. The decay of electron charge density with nitrogen content in the gas stream is measured and seen to occur with the appearance of abundant $N(^2D)$. Strong EPR signals from $N(^2D_{5/2})$ and $N(^2D_{3/2})$ are easily observed; no addition of an electron scavenger, such as SF_6, is necessary for quenching the free electron noise at the resonant cavity [10,12]. The production of metastable atomic nitrogen is explained in terms of the reactions $He_2^+ + N_2 \rightarrow 2He + N_2^+$ followed by $N_2^+ + e \rightarrow N^* + N$.

2. Experimental apparatus

The apparatus employed in our experiments consist essentially of a gas flow line, a microwave discharge system and a commercial X-band EPR spectrometer (Fig. 1).

The gas flow line, built in metal and glass only, is composed of a manifold for mixing the gases, a metal and quartz discharge tube and a pumping system. Each tank is connected to a branch of the manifold through a close-up valve, a needle valve and a linear Teledyne-Hastings linear flow meter; 0-6 sLm for He and 0-50 sccm for N_2. The discharge tube, connected with metallic bellows to the manifold and the pumping line, is made of a quartz tubing with 9 mm and 11 mm inside and outside diameters, except for the glass for metal graded seals. Pressure gauge tubes, which are a distance 1.93 m apart, are connected to the flow line near the ends of the glass tubing; a Teledyne-hastings VH-4 near the manifold and an MKS 227 AHS Absolute Pressure Transducer near the pumps intake. Temperature measurements were made with a Keithley calibrated thermocouple attached to the flow line with a thick insulation wrap. The quartz discharge tube threads the discharge and the spectrometer cavities. A 5 cm long quartz tubing jacket is available for watercooling the flow tube before it enters the X-band cavity.

The pump system consists of three Edwards ES-200, 7 L/s, mechanical pumps, plus a high speed Microvac Stokes 212 H-11, 66 L/s, rotary pump connected in parallel. During experiments, high speed flows are maintained by all of them. The
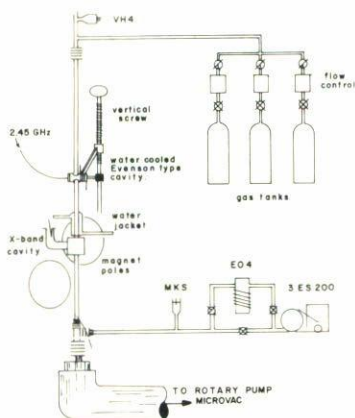
FIGURE 1. Device for measuring electron densities and paramagnetic species in the afterglow of a microwave discharge in fast flowing gases.

flow system was evacuated between experiments with an Edwards E04 oil diffusion pump which can be connected or isolated from the flow line by suitable valves.

The microwave discharge system consists of a Micro-Now 420 B, 2.45 GHz power generator, a flexible transmission coaxial cable and an Evenson-type discharge cavity [13]. This cavity is water cooled with a 1/8" copper tubing coil soldered to its body and it is mounted on a 6 threads/cm, 60 cm long vertical screw by means of which it can be parallely displaced along the discharge tube. Water cooling of this cavity was essential for stable operation and reproducibility.

The EPR spectrometer is an X-band Varian E-112 model equipped with a rectangular, 0.45" × 0.9" × 1.7", Varian E231-2 cavity of 9.5 GHz nominal resonating frequency. The X-band frequency is measured continuously by a Hewlett-Packard 5340-A electronic counter.

3. Free electron density measurements

In a pure helium afterglow, He^+ is the dominant ion at pressures below 1 Torr and room temperature. When the gas pressure is higher than 5 Torr the dominant ion is He_2^+, also at room temperature. For both ionic species the decay in ionization is due to collisional-radiative recombination with very nearly the same recombination coefficient. The assumption of a dissociative recombination mechanism for He_2^+ first proposed was abandoned after years of investigation and many experiments. However the main loss mechanism between the discharge and the resonant cavities is an exponential decay consistent with, as we shall see, ambipolar diffusion to the walls.

Free electrons diffuse in a plasma simultaneously with positive ions. This process is called ambipolar diffusion and results in a diffusion rate approximately equal to

twice that of the much heavier, and slower, positive ion [14]. Ambipolar diffusion of electrons with He^+ is then faster than with He_2^+, the diffusion coefficients being 5.47 m^2-Pa/s and 8.54 m^2-Pa/s respectively [15]. A measurement of the electron ambipolar diffusion coefficient in a helium discharge afterglow can then show which of the above ions is predominant.

This coefficient can be obtained from measurements of the decay of free electron density along the discharge afterglow in a gas flow tube. If the tube radius is much longer than the mean free path for ambipolar diffusion of electrons the electron density may be assumed to vanish at the tube walls with either one of the helium ions and, consequently, to decay exponentially downstream along the tube.

The electron density in the afterglow can be obtained, in principle, from the electron cyclotron resonance curves; the density being proportional to the double integral under these curves. However, on account of the large widths involved, this integral is very sensitive to small deviations of the base line or to distortions of the lineshapes, and yields very inaccurate values not only for absolute, but also for relative measurements at different points in the afterglow. The electron density is best determined from the change Δf induced by the free electrons to the resonant frequency f of the spectrometer X-band cavity. This is so because of the shift depending directly on a weighted average value of the density; as can be seen from the Slater formula

$$\frac{\Delta f}{f} = \frac{e^2}{8\pi^2 \epsilon_0 m} \left(\frac{\int n E^2 dV}{\int E^2 dV} \right), \tag{1}$$

where e is the electron charge, ϵ_0 the free space permittivity, m the electron mass E the microwave electric field and n the number density of free electrons in the cavity [16].

The right hand side of this equation was calculated for a rectangular cavity operating in the TE_{102} mode, traversed by a cylindrical sample tube and assuming an electron number density n with exponential decay along the length of the tube and a parabolic distribution across its diameter; *i.e.*,

$$n = n_0 \exp(-\alpha z) \left[1 - \left(\frac{r}{R} \right)^2 \right], \tag{2}$$

where R is the tube inside radius.

The result of this calculation is

$$\frac{\Delta f}{f} = \frac{e^2}{8\pi^2 \epsilon_0 m} \bar{n} \left(\frac{V_S}{V_C} \right) \frac{1 + 2 \left(\frac{\alpha a}{2\pi} \right)^2}{1 + \left(\frac{\alpha a}{2\pi} \right)^2}$$
$$\times \left(1 - \frac{4d}{3\pi R} J_1 \left(\frac{4\pi R}{d} \right) + \frac{2}{3} {}_1F_2(\tfrac{3}{2}; \tfrac{1}{2}; 3; -(2\pi R/d)^2) \right), \tag{3}$$

where V_S and V_C are the sample and cavity volumes respectively, $\bar{n} = \int n dV / V_S$

$\ln\{(f_o - f')/(f - f')\}$
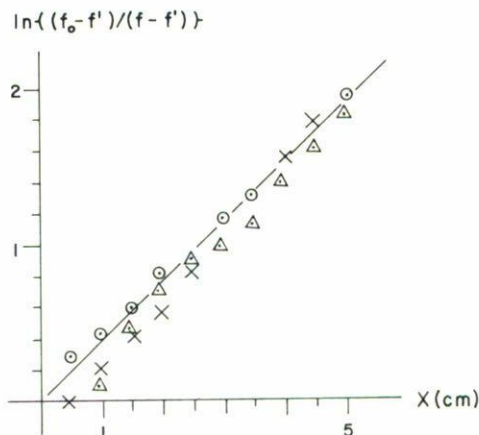
FIGURE 2. Changes in the resonant frequency of an X-band cavity due to changes in the free electron density in the afterglow of a microwave discharge in fast flowing helium.

is the average electron number density in the sample volume, a is the height and d the length of the cavity, J_1 is the first-order Bessel function and $_1F_2$ is a generalized hypergeometric series [17].

For the conditions of our experiment the average electron number density n is given in terms of the frequency shift Δf by

$$\bar{n} = 5.3 \times 10^6 \frac{1 + \left(\frac{\alpha a}{2\pi}\right)^2}{1 + 2\left(\frac{\alpha a}{2\pi}\right)^2} \Delta f. \tag{4}$$

The decay constant α, necessary to calculate n with this equation, was obtained from measurements of the X-band cavity frequency f with distance z along the tube. It can be easily seen that if n changes with z as in Eq. (2), Δf is given in terms of z by

$$f = f' + (f_0 - f')\exp(-\alpha z), \tag{5}$$

where f_0 is the frequency when the discharge is at an arbitrary initial position, for which $z = 0$, and f' is the frequency with the discharge turned off.

In Fig. 2 we show the result of measuring f, f_0 and f' for various positions of the discharge in a convenient form for deducing the value of α for electrons in pure helium. The exponential decay coefficient resulting from this graph, for a helium flow of 2.25 sLpm and a pressure of about 12 kPa at the discharge, is $\alpha = 0.372/\text{cm}$.

Substitution of this value of α in Eq. (4) gives

$$\bar{n} = 5.19 \times 10^6 \Delta f, \tag{6}$$

where Δf is the frequency shift expressed in kHz and $\bar{n}$ the average electron number density in cm^{-3}. With the discharge located 22 cm above the X-band cavity, at a power of about 150 W, the measured frequency shift was $\Delta f = (22 \pm 1.5)$ kHz. This value, substituted in Eq. (6) yields $\bar{n} = (1.14 \pm 0.1) \times 10^8$ cm^{-3}. The electron density at the onset of the afterglow deduced from this value, the distance $z = 22$ cm and $\alpha = 0.372$ cm^{-1} is $n(0) = (4.08 \pm 0.36) \times 10^{11}$ cm^{-3}.

4. Electron ambipolar diffusion coefficient in Helium

Electrons from a helium discharge in a flow line decay primarily by ambipolar diffusion to the walls. The speed at which any initial electron distribution relaxes to the fundamental mode diffusion distribution depends only on, but is a very slow function of the parameter $\beta = \alpha_r n \Lambda^2 / D_a$, where α_r is the helium recombination rate coefficient, n is the free electron density, Λ is the diffusion length and D_a is the ambipolar diffusion coefficient [18]. For large values of β, over 100, the electron distribution departs appreciably for short times from the fundamental mode distribution. In our experiment, however, $\alpha_r(\text{He}) < 10^{-8}$ cm^3/s, $n \approx 10^{11}$ cm^{-1}, $\Lambda = R/\lambda_1 = 0.19$ cm and $D_a > 58$ cm^2/s. These values make $\beta < 1$ for any helium ionic species. We can then expect the process to be diffusion controlled and the electron distribution to be already in the fundamental mode at a few centimeters from the discharge. The electron density will then decay along the tube like $\bar{n} = \bar{n}_0 \exp(-\alpha z)$, where $\alpha = D_a \lambda^2 / (2R^2 u_0)$, $D_a = D_0/p$ is the ambipolar diffusion coefficient at pressure p, R is the tube inside radius, u_0 is the mean-flux velocity in Poiseuille viscous flow equation and $\lambda_1 = 0.2710$.

The value of the electron ambipolar diffusion coefficient in helium can then be obtained from a measurement of the electron number density decay coefficient α as given above. It is more convenient, however, to express α in terms of the flow of mass $Q = \rho(\pi R^2)u_0$, where ρ is the gas density. In terms of this quantity the relation between D_0 and α is

$$D_0 = 14.64 \alpha Q, \tag{7}$$

where D_0 is expressed in m^2-Pa/s, α in cm^{-1} and Q in sLpm.

Substituting the values $\alpha = 0.372$ cm^{-1} and $Q = 2.25$ sLpm we obtain $D_0 = 12.25$ m^2-Pa/s for ambipolar diffusion in helium at 340 K; or, taking into account the T^2 dependence at constant pressure, $D = 9.09$ m^2-Pa/s at room temperature [15]. Comparing with the known values at room temperature, $D_0(He_2^+) = 8.54$ m^2-Pa/s and $D_0(He^+) = 5.47$ m^2-Pa/s, we see that He_2^+ is dominant in our helium discharge

5. Free electron density in a He-N$_2$ discharge

We also observe the changes in electron density induced in a helium afterglow as small amounts of nitrogen are added to the flow discharge. In this case, we measured
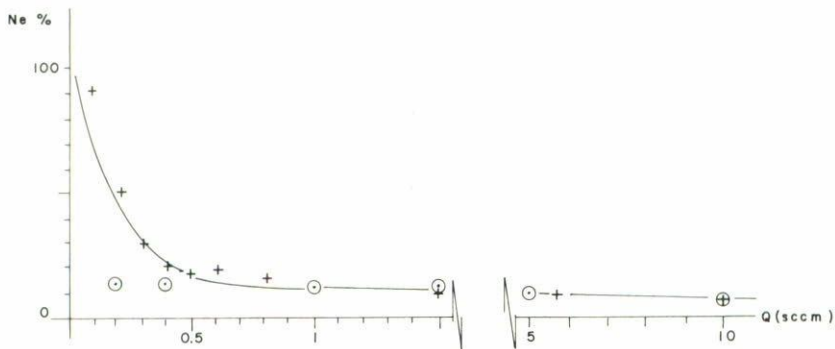
FIGURE 3. Decay of free electron density in a helium gas discharge as a function of concentration
of added nitrogen. Helium flow is equal to 2.25 sLm.
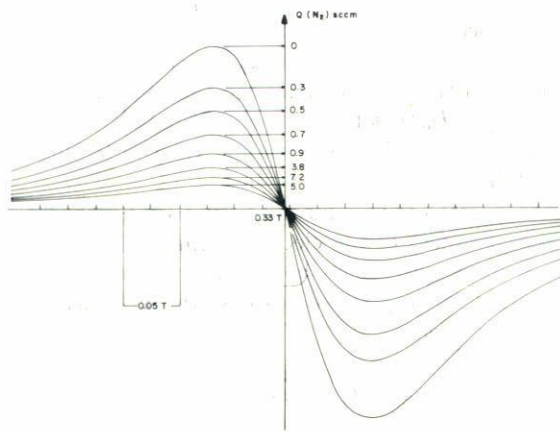
FIGURE 4. Decay of electron cyclotron resonance signals, as observed by EPR, as a function of
added nitrogen. Helium flow is 2.25 sLm.

the electron density from the changes induced by free electrons to the X-band cavity
frequency and from the relative intensities of the electron cyclotron resonance ab-
sorption lines (Figs. 3 and 4). In this method, the intensities were taken proportional
to the second integral of the cyclotron resonances as obtained by numerical integra-
tion in an on-line computer (Varian E-900 Data Acquisition System). Fig. 3 shows
the free electron density, at a point 17 cm downstream from cavity, as a function
of the N_2 flow. Molecular density values are also shown. These were calculated on
the assumption that, on account of the comparatively small nitrogen flow, the N_2

velocity is equal to the helium velocity. The nitrogen molecular density can then be deduced from the equation

$$\frac{n(N_2)}{Q(N_2)} = \frac{n(He)}{Q(He)}, \tag{8}$$

where n and Q are the molecular density and the gas flow, respectively.

Free electron density in a helium afterglow decreases rapidly with increasing partial pressure of N_2 in the helium discharge. With molecular nitrogen present in the discharge and in the afterglow, the dissociative recombination process

$$N_2^+ + e \rightarrow N^* + N \tag{9}$$

is available. This recombination process is orders of magnitude faster than the collisional-radiative and represent the main loss mechanism in the afterglow. However, as is known, the dissociative-recombination coefficient varies with temperature T_e as $T_e^{-1/2}$ [19]. We can then assume that all electrons are first thermalized and only then they recombine with N_2^+ dissociatively. For He_2^+ and He^+, as noted above, the recombination process is the very much slower collisional-radiative. In fact, recent theoretical and experimental work [20,21] in electron thermalization in Ar-N_2 and Xe-N_2 gas mixtures shows that the contribution of N_2 to the total energy-loss rate in the mixture (with 0.01 N_2 fraction), represents more than 85% of the energy-loss rate, due to the many efficient rotational and vibrational states available in molecular nitrogen.

Another very important quenching mechanism in the afterglow with N_2 present is the charge transfer process [22]

$$He_2^+ + N_2 \rightarrow N_2^+ + 2He. \tag{10}$$
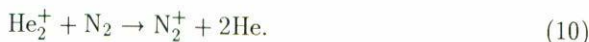
As we will see in the next section, this process in the He-N_2 afterglow plays the role of an electron scavenger of SF_6 in the experiments of Diebold *et al.* [10,12], which led to the EPR observation of nitrogen metastables.

6. Metastable atomic nitrogen in the discharge afterglow

$N(^2D)$ *spectra.* Metastable atomic nitrogen, $N(^2D)$, has been observed in the products of a microwave discharge in He-N_2 by EPR only in hypersonic flow of the gas mixture in very critical conditions [7,8] or by introducing SF_6 in the afterglow as an electron scavenger to reduce the free electron noise in the EPR cavity to tolerable levels [10,12]. The results of Figs. 5 and 6 indicate, however, that the $N(^2D)$ spectra could also be observed by taking advantage of the electron scavenging properties of N_2 itself. We were able, indeed, to observe these spectra at a range of He and N_2 partial pressures, with He pressure above 0.666 kPa and 5% of N_2 partial pressure. Figs. 5 and 6 shows, both, the $^2D_{5/2}$ and the much weaker $^2D_{3/2}$ spectra. Further addition of SF_6 to the afterglow brought no improvement to the observed spectra.

Spectrum of $N^*(^2D_{5/2})$

FIGURE 5. N($^2D_{5/2}$) EPR spectrum observed in the afterglow of a He-N$_2$ microwave discharge.

Spectrum of $N^*(^2D_{3/2})$
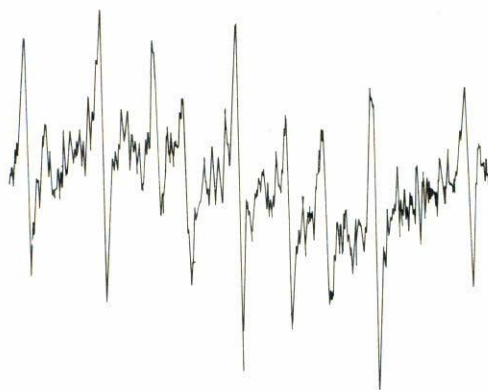
FIGURE 6. N($^2D_{3/2}$) EPR spectrum observed in the afterglow of a He-N$_2$ microwave discharge.

N(^2D) *production.* Metastable and ground state atomic nitrogen are produced in the discharge mainly by dissociative recombination process

$$N_2^+ + e \rightarrow N^* + N. \tag{9}$$

The two main excited helium species present in the discharge are the molecular ion He$_2^+$, and the 2^3S metastable atomic helium He*. Either one of these can react with N$_2$ to yield the electronically excited N$_2^{+*}$. The corresponding reactions are the

charge transfer process

$$He_2^+ + N_2 \rightarrow 2He + N_2^{+*}, \tag{10}$$

and the Penning reaction

$$He^* + N_2 \rightarrow He + N_2^{+*} + e. \tag{11}$$
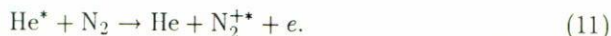
N_2^{+*} decays then immediately to N_2^+ by emission of a light quantum

$$N_2^{+*} \rightarrow N_2^+ + h\upsilon. \tag{12}$$

The resulting N_2^+ ion rapidly recombines dissociatively producing more N^* atoms and quenching the free electron plasma. Of central importance is the fact that He_2^+ be the dominant helium ion, as certainly happens at pressures we are working with. Moreover, at our working pressures, it is well known that about 70% of the He_2^+ ions leads to the production of atomic triplet helium metastables [15], suggesting the above reactions at our gas pressures. The role of small concentration of nitrogen in a helium discharge can then be described as follows. First, it thermalizes the free electrons in the discharge. Secondly, it catalyzes the recombination of He_2^+ *via* a charge transfer process (Eq. 10). Finally, it produces atomic metastables N^* by fast recombination with free electrons (Eq. 9).

7. Conclusions

We find that adding N_2 in small amount to a microwave discharge in helium drastically reduces the free electron density in the afterglow to a few percent of its initial value. The effect is comparable to that of traditional electron scavengers like SF_6., but while this compound works in the relatively cold afterglow proceeding from the formation of SF_6^- to the charge neutralization of He^+, nitrogen must go through the discharge itself in order to produce similar effects. This is, indeed, indicative of the role of N_2^+ in the process of charge neutralization by nitrogen.

The free electron scavenging properties of nitrogen can certainly be employed to reduce electron noise in gas phase EPR; in this work it has been used to observe the metastable atomic nitrogen EPR spectra. However, since it is added to the discharge itself; it may interfere with the kinetics of reacting species which would, otherwise, be produced by the discharge.

Acknowledgement

References

1. S. Krongelb and M.W.P. Strandberg, *J. Chem. Phys.* **31** (1959) 1196.
2. A.A. Westenberg and N.H. de Haas, *J. Chem. Phys.* **40** (1964) 3087.
3. K.M. Evenson and D.S. Burch, *J. Chem. Phys.* **45** (1966) 2450.
4. R. Beringer and E.B. Rawson, *Phys. Rev.* **87** (1952) 228.
5. E.B. Rawson and R. Beringer, *Phys. Rev.* **88** (1952) 677.
6. M.A. Heald and R. Beringer, *Phys. Rev.* **96** (1954) 645; V. Beltrán-López, J. Rangel G., A. González N., J. Jiménez-Mier, and A. Fuentes M., *Phys. Rev.* **A39** (1989) 58.
7. K.M. Evenson and H.E. Radford, *Phys. Rev. Lett.* **15** (1965) 916.
8. H.E. Radford and K.M. Evenson, *Phys. Rev.* **168** (1968) 70.
9. G.J. Diebold, I.V. Rivas, S. Shafeizad and D.L. McFadden, *J. Chem. Phys.* **52** (1980) 453.
10. G.J. Diebold and D.L. McFadden, *Rev. Sci. Instrum.* **50** (1979) 157.
11. M.A. Biondi, *Rev. Sci. Instr.* **22** (1951) 500.
12. G.J. Diebold and D.L. McFadden, *Phys. Rev.* **A25** (1982) 1504.
13. F.C. Fehsenfeld, K.M. Evenson and H.P. Broida, *Rev. Sci. Instr.* **36** (1965) 294.
14. M.A. Biondi and S.C. Brown, *Phys. Rev.* **75** (1949) 1700.
15. R. Deloche, P. Monchicourt, M. Cheret and F. Lambert, *Phys. Rev.* **A13** (1976) 1140.
16. J.C. Slater, *Rev. Mod. Phys.* **18** (1946) 481.
17. I.S. Gradshteyn and I.M. Ryzhik, *Table of Integrals, Series and Products.* Academic Press, New York (1965).
18. E. P. Gray and D.E. Kerr, *Annals of Physics* **17** (1959) 276.
19. J.N. Bradsley and M.A. Biondi, *Adv. in Atomic and Molec. Physics* **6** (1970) 1.
20. B.L. Tembe and A. Mozumder, *Phys. Rev.* **A27** (1983) 3274-3278; *J. Chem. Phys.* **78**(1983) 2030.
21. A. Mozumder, *J. Chem. Phys.* **72** (1980) 1657.
22. Collins and Robertson, *J. Chem. Phys.* **40** (1964) 701, 2202 and 2208.

Resumen. Observamos átomos de nitrógeno metaestable $N(^2D)$ y electrones libres, en el resplandor de una descarga de micro-ondas en una corriente de gas He-N_2, por medio de EPR. Las densidades de electrones libres fueron medidas a partir de los corrimientos de la frecuencia en la cavidad en banda-X del espectrómetro.

En el resplandor de la descarga con helio puro, a 363 K, con presiones por arriba de 6.5 kPa, se midió el decaimiento en la densidad de electrones libres con la distancia. A partir del valor obtenido en estas medidas para la constante de difusión ambipolar, se demostró que el He_2^+ predomina sobre el He^+ en el resplandor.

Se observó que la densidad de electrones libres decae en el resplandor conforme se agrega N_2 a la corriente gaseosa, midiéndose dicha densidad como función del flujo de N_2. Fueron observadas fuertes señales EPR de $N(^2D)$, con un 5% de presión parcial de nitrógeno. La producción de $N(^2D)$ por reacciones $He_2^+ + N_2 \rightarrow 2He + N_2^+$, seguidas por $N_2^+ + e \rightarrow N^* + N$, quedan evidenciadas por estas medidas.